

## Crystallographic Analysis of an 8-mer p53 Peptide Analogue Complexed with MDM2

Kaori Sakurai,<sup>†</sup> Carsten Schubert,<sup>‡</sup> and Daniel Kahne<sup>\*,†,§</sup>

Department of Chemistry and Chemical Biology, Harvard University, 12 Oxford Street, Cambridge, Massachusetts 02138, Johnson & Johnson Pharmaceutical Research & Development L.L.C., 665 Stockton Drive, Exton, Pennsylvania 19341, and Department of Biological Cellular and Molecular Pharmacology, Harvard Medical School, Longwood, Boston, Massachusetts 02115

Received May 3, 2006; E-mail: kahne@chemistry.harvard.edu.

MDM2 is a regulator of a tumor suppressor p53, which protects cells by responding to genotoxic stresses with an induction of cell cycle arrest or apoptosis.<sup>1</sup> Because downregulation of p53 by overexpression of MDM2 has been implicated in many human cancers, there has been a great interest in exploiting the p53–MDM2 interface as a chemotherapeutic target.<sup>1–3</sup> The molecular details of the interface was revealed by X-ray crystallographic studies.<sup>4</sup> MDM2 recognizes the three conserved hydrophobic residues (Phe19, Trp23, and Leu26) within a 15-residued N-terminal region of the p53 transactivation domain (Figure 1, **1**). The side chains of the key p53 residues form a hydrophobic binding motif on one face of a short  $\alpha$ -helix, which fits tightly to the hydrophobic cleft of MDM2. More recently, small molecule inhibitors (Figure 1, **3,4**) with superior potency to that of the wt-p53 peptide ligand **1** were discovered through chemical library screening.<sup>5,6</sup> The crystal structures of their MDM2 co-complexes showed that relatively simple hydrophobic functionalities can fill the MDM2 pocket. The most potent MDM2 inhibitor reported to date is an 8-residue p53 peptide analogue **2** (Figure 1,  $IC_{50} = 5$  nM).<sup>7</sup> It was developed by the Novartis group through rational design based on a peptide sequence derived from a phage-display library<sup>8</sup> and the X-ray structure of **1** bound to MDM2.<sup>3</sup> **2** has been shown to restore the p53 function in cells harboring wt-p53 and overexpressed MDM2.<sup>9</sup> We describe herein the co-complex structure of **2** and MDM2 at 1.8 Å resolution by X-ray crystallography. Two aromatic residues, 6-chlorotryptophane (Cl-Trp) and phosphonomethylphenylalanine (Pmp) were previously shown to be principally responsible for the elevated MDM2 binding affinity of **2**.<sup>7–10</sup> The co-complex structure provides new insights into the roles of these two residues.

The 8-mer peptide **2** was synthesized as diastereomers (using a racemic Cl-Trp residue) and was then isolated by HPLC as reported.<sup>7</sup> Crystals were successfully obtained only for one of the diastereomers as a complex with MDM2 by vapor diffusion using the hanging drop method. The structure was solved by molecular replacement as implemented in CNX using the structure of MDM2 bound to a 9-mer p53 peptide analogue<sup>6</sup> as a search model. The ligand-bound MDM2 forms a deep hydrophobic cleft with a pair of two  $\alpha$  helices packed by a pair of three stranded  $\beta$  sheets in a similar manner as found previously for the complex with **1** (Supporting Information, Figure S1). The peptide analogue **2** forms short  $\alpha$ -helical turns in the hydrophobic cleft of MDM2, occupying the same site where the Phe19–Leu26 region of **1** binds. The two MDM2 co-complex structures have a root-mean-square deviation (RMSD) of 0.60 Å for equivalent  $\alpha$ -carbon atoms. These ligand-bound MDM2 structures are also very similar to other crystal

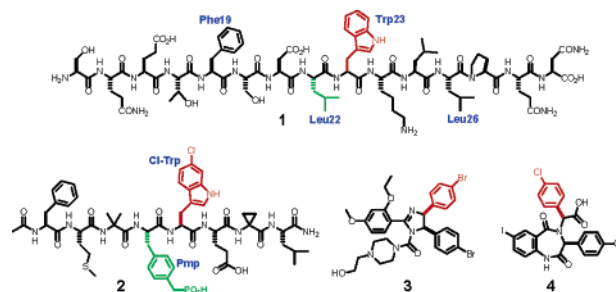


**Figure 1.** Structures of MDM2 inhibitors: **1**, the 15-mer wt-p53 peptide ( $IC_{50} = 4 \mu M^{3a}$ ); **2**, the 8-mer peptide analogue (Novartis peptide,  $IC_{50} = 5$  nM<sup>7</sup>); **3**, imidazoline-based peptidomimetics (Nutlin-2,  $IC_{50} = 140$  nM<sup>5</sup>); **4**, benzodiazepinedione-based peptidomimetics ( $K_d = 80$  nM<sup>6</sup>). Functional groups that bind to the Trp binding site of MDM2 are highlighted in red. Leu 22 and Pmp are highlighted in green.

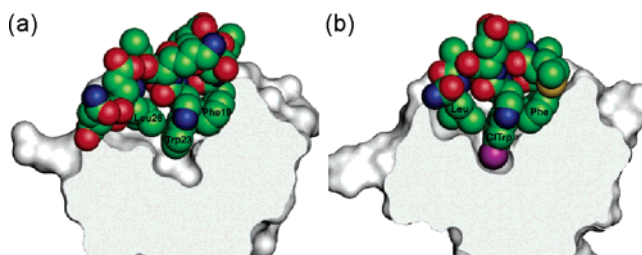


**Figure 2.** A cutaway view of the MDM2 Trp binding site (grey surface) with (a) the bound wt-p53 peptide **1** and (b) the bound 8-mer peptide analogue **2** (Novartis peptide) shown as CPK models. The Cl atom of the Cl-Trp residue is highlighted in magenta. Panels a and b show identical orientations. Images are rendered in Pymol.

structures of inhibitor-bound MDM2,<sup>5,6</sup> in contrast to recent NMR studies suggesting that different ligands induce different conformational transitions in the protein.<sup>11</sup> Our results thus support the validity of using the ligand-bound MDM2 conformation determined by X-ray crystallography as a guide for inhibitor design.

In the complex, peptide **2** forms conserved hydrophobic interactions with MDM2 at residues Phe, Cl-Trp, and Leu.<sup>12</sup> Each of the three hydrophobic residues of **2** is accommodated in the same p53 binding site of the MDM2 pocket (Leu54, Leu57, Gly58, Ile61, Met 62, Tyr67, Gln72, His73, Val93, His96, Ile99, and Tyr100) as those in **1**. The N1–H of Cl-Trp is engaged in a hydrogen bonding interaction with the backbone amide group of MDM2 Leu54 as observed between Trp23 of **1** and MDM2 Leu54. Thus, the peptide **2** binds virtually identically to the wt-p53 peptide **1**.

The importance of the Cl atom in MDM2 binding becomes evident when the complex of **2** is compared to the complexes of wt-p53 peptide **1** (Figure 2), and of the nonpeptidic inhibitors **3** and **4** (Figure 3). As initially predicted,<sup>7</sup> the 6-Cl atom of the Cl-Trp residue of **2** protrudes into a void of the Trp23 binding site of

<sup>†</sup> Harvard University.

<sup>‡</sup> Johnson & Johnson Pharmaceutical Research & Development L.L.C.

<sup>§</sup> Harvard Medical School.



**Figure 3.** An overlay of the **2** (yellow stick)–MDM2 cocomplex with **3** (blue stick) and **4** (green stick) bound to the corresponding sites. The Cl atoms are colored in magenta and the Br atom in orange. For **2**, side chains of only Phe, Cl-Trp, and Leu are shown for clarity. MDM2 is shown with a cutaway surface (grey).

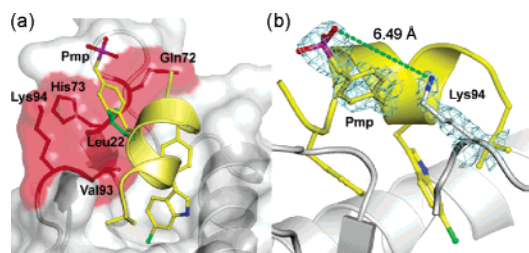


**Figure 4.** Shown are two views showing the Pmp binding site. (a) The Pmp residue of **2** (yellow) makes hydrophobic contacts to the MDM2 residues (highlighted in red) in a similar manner to Leu 22 (green stick) of **1**. (b) Distance between Pmp and Lys94 is outside the range of a salt bridge. Shown is a 2Fo-Fc electron density map contoured at  $1.4\sigma$  and rendered as blue mesh within  $2\text{ \AA}$  of the side chains of Pmp and Lys94. One of the two rotamers observed for the phosphonate group is shown for simplicity.<sup>16</sup>

MDM2, making additional van der Waals contacts with Phe86 and Ile99 (Figure S2). As a result, the steric complementarity at the protein–peptide interface is highly optimized (Figure 2). The positions of the Cl atom of **2**, the Br atom of **3**, and the Cl atom of **4** are superimposable in the MDM2 pocket, even though the scaffold structures are different (Figure 3).<sup>13</sup> In all three structures, the rigid aromatic moieties position the halogen atoms deep into the cavity at the bottom of the Trp binding site. A structural isomer of **3**, which bears a Cl atom instead of a Br atom at the same position, displays an augmented MDM2 inhibitory potency than **4**,<sup>5</sup> suggesting that chlorine is the ideal size to fill the cavity. Chlorine has a van der Waals radius of  $1.8\text{ \AA}$ , and there is no other organic functionality of an equivalent size. Chlorinated aromatic groups are present in most of known small molecule MDM2 inhibitors.<sup>2,3e–f,14</sup>

While the structure of the co-complex verifies the predicted role of Cl in binding to MDM2, it suggests that the Pmp residue plays a different role than proposed. Figure 4 shows that the side chains of Leu22 and Pmp contact Gln72, His73, and Val93 of MDM2 in a similar orientation, preserving key hydrophobic interactions.<sup>4,15</sup> The Pmp residue, is thought to contribute significantly to the greater affinity of **2** compared with **1**, which contains leucine at the same position, and was proposed to make an electrostatic contact to the  $\epsilon$ -amino group of the MDM2 Lys94.<sup>7</sup> However, the phosphonate group of the Pmp residue does not form the predicted salt bridge, but instead projects into the solvent.<sup>16</sup> To examine the importance of the phosphonate group in binding to MDM2, we prepared an analogue of **2** containing Phe (peptide **5**) in place of the Pmp residue and compared the binding of the two peptides using a previously reported ELISA assay.<sup>3a</sup> The affinity of peptide **5** was reduced by only 2-fold compared with that of peptide **2** (Supporting Information), consistent with the X-ray structure showing that the phosphonate does not interact with any protein side chains. **5** shows a greater tendency to aggregate compared with **2** (as judged by NMR

linewidths and its insolubility in pH 7 phosphate buffer at millimolar concentration), which may account for its somewhat lower binding affinity.

In conclusion, we have determined the atomic structure of the most potent MDM2 inhibitor identified to date.<sup>17</sup> The interaction is clearly dominated by binding of conserved hydrophobic residues Phe, Cl-Trp, and Leu of **2**, as expected on the basis of the binding of peptide **1** to MDM2. The structure reveals the importance of the chlorine atom in filling the cavity at the base of the Trp binding pocket. The structure also shows that the phosphonate of the Pmp residue does not participate in direct contact with the protein, as previously proposed. Although studies of other model peptides have suggested that the Pmp residue plays a significant role in binding, we have shown that the Pmp residue can be replaced by Phe (**5**) with only a 2-fold loss in affinity. Evidently, the results obtained during iterative optimization of model peptides do not apply to the fully optimized peptide sequence, illustrating the limitations of iterative optimization procedures with respect to the importance of individual residues in the final system.

**Acknowledgment.** This work was supported by National Institutes of Health Grant 69721 and 3-Dimensional Pharmaceutical Inc. We thank Diane Maguire for her work on the protein preparation.

**Supporting Information Available:** Material and methods, supplementary figures, X-ray data processing, structure refinement statistics, and complete references for ref 3c, 3f, 5, 6, and 14. This material is available free of charge via the Internet at <http://pubs.acs.org>.

## References

- (1) (a) Vogelstein, B.; Lane, D.; Levine, A. *J. Nature* **2000**, *408*, 307. (b) Chène, P. *Nat. Rev. Cancer* **2003**, *3*, 102.
- (2) For a recent review of small molecule MDM2 inhibitors, see Fischer, P. M.; Lane, D. P. *Trends Pharmacol. Sci.* **2004**, *25*, 343.
- (3) For recent efforts on the design of MDM2 inhibitors based on peptidomimetic scaffolds, see (a) Sakurai, K.; Chung, H.-S.; Kahne, D. *J. Am. Chem. Soc.* **2004**, *126*, 16288. (b) Yin, H.; Lee, G. I.; Park, H. S.; Payne, G. A.; Rodoriguez, J. M.; Sebt, S. M.; Hamilton, A. D. *Angew. Chem., Int. Ed.* **2005**, *44*, 2704. (c) Gellman, S. H.; et al. *J. Am. Chem. Soc.* **2005**, *127*, 13271. (d) Kritzer, J. A.; Leudtke, N. W.; Harker, E. A.; Schepartz, A. *J. Am. Chem. Soc.* **2005**, *127*, 14584. (e) Hara, T.; Durell, S. R.; Myers, M. C.; Appella, D. H. *J. Am. Chem. Soc.* **2006**, *128*, 1995. (f) Robinson, J. A.; et al. *ChemBioChem* **2006**, *7*, 515.
- (4) Kussie, P. H.; Gorina, S.; Marechal, V.; Elenbaas, B.; Moreau, J.; Levine, A. J.; Pavlitch, N. P. *Science* **1996**, *274*, 948.
- (5) Vassilev, L. T.; et al. *Science* **2004**, *303*, 844.
- (6) Grasberger, B. L.; et al. *J. Med. Chem.* **2005**, *48*, 909.
- (7) Garcia-Echeverria, C.; Chène, P.; Blommers, M. J. J.; Furet, P. *J. Med. Chem.* **2000**, *43*, 3205.
- (8) Böttger, V.; Böttger, A.; Howard, S. F.; Picksley, S. M.; Chène, P.; Garcia-Echeverria, C.; Hochkeppel, H. K.; Lane, D. P. *Oncogene* **1996**, *13*, 2141.
- (9) Chène, P.; Fuchs, J.; Bohn, J.; Garcia-Echeverria, C.; Furet, P.; Fabbro, D. *J. Mol. Biol.* **2000**, *299*, 245.
- (10) Substitution of Trp by Cl-Trp led to a 60-fold increase in the inhibitory potency. A mutation Leu22Tyr in a 12-mer p53 peptide (Gln16–Pro27) was favorable by 10-fold, while replacing Tyr by Pmp enhanced the potency by 7-fold in an isomer of **2**, which contains Trp instead of Cl-Trp (see ref 7 and ref 8).
- (11) (a) Schon, O.; Friedler, A.; Bycroft, M.; Freund, M. V.; Fersht, A. R. *J. Mol. Biol.* **2002**, *323*, 491. (b) Schon, O.; Friedler, A.; Freund, S.; Fersht, A. R. *J. Mol. Biol.* **2003**, *336*, 197. (c) Uhrinova, S.; Uhrin, D.; Powers, H.; Watt, K.; Zheleva, D.; Fischer, P.; McInnes, C.; Barlow, P. N. *J. Mol. Biol.* **2005**, *350*, 587.
- (12) The C $\alpha$  stereocenter of the Cl-Trp residue was unambiguously determined to be S (L).
- (13) The Cl atom of Cl-Trp presented on a  $\beta$ -hairpin scaffold also binds to the Trp binding site of MDM2 in a similar fashion (see ref 3f).
- (14) Wang, S.; et al. *J. Am. Chem. Soc.* **2005**, *127*, 10130.
- (15) (a) Lin, J.; Chen, J.; Elenbaas, B.; Levine, A. J. *Genes Dev.* **1994**, *15*, 1235. (b) Massova, I.; Kollman, P. A. *J. Am. Chem. Soc.* **1999**, *121*, 8133.
- (16) Two rotamers around the C–P bond observed for the phosphonate groups in the complex, respectively, make different patterns of water-mediated hydrogen bonds to the MDM2 residues (Figure S3). Although unlikely, we cannot exclude the possibility that they may contribute to the increased stabilization of the MDM2–peptide interaction.
- (17) Coordinates for the structure have been deposited with the RCSB Protein Data Bank (PDB access code 2GV2).

JA063102J